Designing a High Performance Humanoid Robot Based on Dynamic Simulation

Houman Dallali, Mohamad Mosadeghzad, Gustavo Medrano-Cerda, Vo-Gia Loc, Nikos Tsagarakis, Darwin Caldwell
Department of Advanced Robotics, Istituto Italiano di Tecnologia (IIT) via Morego, 30, 16163 Genova, Italy.
Email: houman.dallali@iit.it

Michele Gesino
iCub Facility, Istituto Italiano di Tecnologia (IIT) via Morego, 30, 16163 Genova, Italy.
Email: michele.gesino@iit.it

***Abstract*—In this paper, we present a study on dynamic simulation to assist designing a high performance compliant humanoid robot. An open source dynamic simulator is introduced which includes the rigid body and actuator dynamics of the full humanoid robot. A set of representative tasks for humanoid robot in rescue operations are chosen and simulated. The data from these tasks are used in sizing the motor and transmission gear for each joint of the robot. It is shown that in the representative tasks, the most critical joint of the robot (in terms of power consumption) is the knee joint. Furthermore, a recently proposed optimization method is used to obtain the value of passive compliance for each joint. The data obtained from simulation studies are used for designing the new humanoid robot.**

***Keywords*-Humanoid Robot; Dynamic Simulation; Walking; Design Requirements;**

I. Introduction

The recent Fukushima accident showed the demand for use of robots for surveillance and tele-operation in hazardous environments. During this accident, mobile and aerial robots were used for surveillance inside various parts of the Fukushima nuclear plant and also for detection of 'hot-spot' areas where humans should avoid for safety.

Following recent advances in humanoid robots, many robotics research groups believe that humanoids can also assist in such scenarios, providing more dexterity and agility. Numerous robots are being built around the world in various creative morphologies with high performance and high robustness properties [1]. Dynamic simulation tools are used by many groups to obtain the design parameters. The Lola humanoid robot was designed by optimizing the topologies and deriving torque-speed characteristics for the leg joints [2]. Ideas from limit cycle walking was used to design Flame and Tulip compliant bipedal robots [3]. In [4], optimal control was used for actuator selection of bipedal robots.

The design philosophy in this study is to use passive compliance and series elastic actuators. The main advantage is to provide protection to the robot joints against shocks from interactions with the environment. The passive compliance can react immediately to impacts while the active impedance can be used to provide a more controlled and stiff motion for the robot.

In rescue robotics the robot must travel over uneven terrain, move rubble and debris from doorways, and lift power tools to be used in tele-operation. However, considering all these scenarios is quite complicated in terms of obtaining design requirements. However, any complex motion can be decomposed into a set of simplified task primitives for the purpose of quantifying power and speed requirements. These simplified motions include walking, step up, squat (with one or both legs), push up (to quantify quadruped motion), pull up (in climbing a ladder) motions. Simulating the robot motion in the mentioned tasks can provide a good estimate of the required power and speed at each joint.

This paper presents the results of compliant joint dynamic simulations to design a rescue humanoid robot. The starting point for the design of this robot is based on the existing humanoid robot COMAN [5] developed at the department of advanced robotics in Istituto Italiano di Tecnologia (IIT). The main goal of the design is to build a compliant humanoid robot with high capability and robustness to assist in a real disaster situation.

The development of this high performance humanoid robot is undertaken in the European Walkman project [6], and aims at designing and building an anthropomorphic robotic platform capable of operating outside the laboratory in unstructured environments and work spaces arising in natural and man-made disasters. In this study, we specifically seek to answer three questions. First, what torque-speed range should be available for each joint of the robot. Second, what kinematic range of motion is needed for the joints. Third, what spring values should be selected for improved compliance performance of the robot.

This paper is organized as follows. Section II, gives an overview of the open source COMAN Simulator. The simplified subtasks are described in section III. Section IV, presents the design requirements for the humanoid robot obtained from simplified dynamic simulations. Finally, conclusions are given in Section V.

II. The Compliant Joint Dynamic Simulator

This section provides an overview of the recently released open source Compliant joint simulator [7], [8], which is

978-1-4799-2578-0/13 $31.00 © 2013 IEEE
DOI 10.1109/EMS.2013.61

based on Robotran multi-body modeling tool [9]. This simulator uses the mathematical equations of the 23 DoF (Degrees of Freedom) COMAN robot (Newton-Euler), generated and optimized symbolically as opposed to numerical models. Subsequently, the actuator dynamics are added to the multi-body model, which consists of the electrical and mechanical dynamics of DC motors. Moreover, constraints, external forces (feet-ground interaction), as well as symbolic kinematic sensors are available to obtain Jacobian, linear and angular position, velocity and acceleration at any point of interest on the humanoid robot.

All equations are generated in C and Matlab languages to leverage the power of Matlab during the development stage and the flexibility of C in the final dissemination. The parameters of COMAN used in the simulations are obtained from the CAD data and the actuator manufacturers data. The complete open source code of the simulator is available for download from the public git repository at [14] for research purposes under GNU license. The generated C code is executed in Linux operating systems independent from Matlab for real-time experimentation. The development of this simulator is still ongoing and so far it has been used in a number of dynamic simulation studies [11], [12] and [13]. Further details regarding the development of the model and simulator can be found in [7] and [10].

III. Task Descriptions

This section, discusses the tasks primitives that can help in estimating the required speed and torque for each joint. The compliance values are fixed at this stage, using the initial values for COMAN [5]. The tasks trajectories are first specified in Cartesian space, converted to joint space using inverse kinematics and then the full body dynamics is simulated using a Runge-Kutta solver. The following naming convention is used for convenience when referring to different DoFs: Ankle (A), Knee (K), Hip (H), Waist (W), Shoulder (S), Elbow (E). Also the rotations Roll, Pitch and Yaw are abbreviated as R, P, Y, respectively. The graphs of this simulation are presented at the end of this section. The data presented in the following sections is presented in a statistical sense. For every joint, the box in each figure corresponds to steady state values of speed or torque. The line inside the box represents the median while the box upper and lower edges are the 25th and 75th percentiles of the torque or speed values. Peak values occurring during transients are shown by the dashed lines. The transient values are less frequent compared to the steady state values during any task.

A. Task 1: Pull Up

Fig. 1 shows the pull up task. This motion demands high torque and power in elbow and shoulder pitch joints during raising motion. The task is designed to lift the legs by 30 cm from the ground. Moreover, Elbow motors should bear the high torque of body weight around hand's arm. This task can resemble climbing a ladder, pulling debris blocking an entrance. The plot of this case is depicted in Fig. 2.

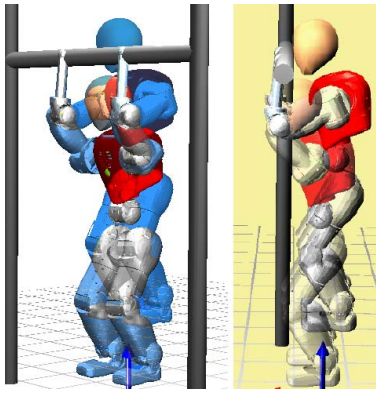

Figure 1. Pull Up

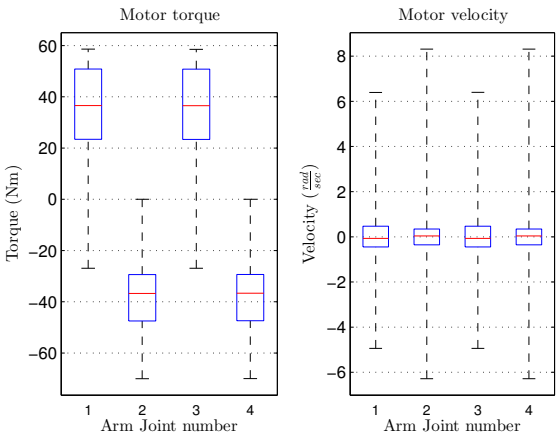

Figure 2. torque-velocity distributions of pull up motion. Joints 1, 2, 3 and 4 refer to SP, E of right and left arms, respectively.

B. Task 2: Push Up

Fig. 3 depicts the push up motion. This task validates motor abilities of ankle, knee, waist pitch and also elbow and shoulder. This task corresponds to quadruped locomotion and also standing up when falling. The quadruped locomotion is more stable in unstructured environments. Hence a humanoid rescue robot should be able to perform well and robustly on four limbs as well as two limbs. The trajectory used for the arm joints is $r(t) = -0.4 + A(1 - cos(2\ \pi\ f\ t))$ where $f = 1\ Hz$ and $A = 0.3\ rad$ and the data is depicted in Fig. 4.

C. Task 3: Step Up

This task is subtask of walking on rough terrain in natural disasters where there is debris on the path of the

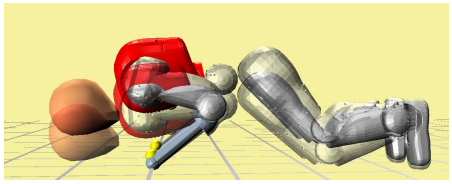

Figure 3. Push Up

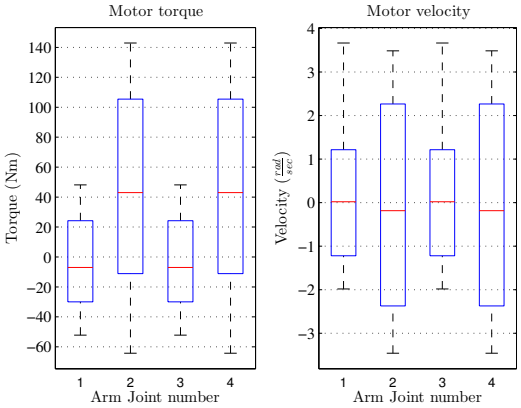

Figure 4. torque-velocity distributions of push up (arms). Joints 1, 2, 3 and 4 refer to SP, E of right and left arms, respectively.

robot. Moreover climbing an industrial ladder, ascending and descending stair cases require strong knee and hip motors. Fig. 5 illustrates the stepping on an obstacle. In this simulation, the robot takes a step over a 30 cm high obstacle which needs high torque and power in knee and hip joints. The plot of this case is depicted in Fig. 6, which is derived for the simulation duration of 6 seconds.

D. Task 4: Squat

Squat is another subtask which arises in many situations such as lifting heavy loads, the transition from bipedal to quadrupedal configuration, walking in confined spaces where there is a low ceiling. Squat demands high torque in knee and hip and becomes harder when the knee bends to π rad. Two set of squat tests are simulated with the robot. First, the robot is simulated to squat symmetrically with both legs with the reference position being $r(t) = A(1-cos(2\,\pi\,f\,t))$, with $f = 1\ Hz$ and $A = 0.3\ rad$ for HP, AP joints and $A = 0.6\ rad$ for knee joint. Second, the robot is simulated to do a squat with one leg while the trajectory is $r(t)$ with the swing leg lifting up twice the stance leg with the same frequency. The plots of the two cases are depicted in Fig. 7 and Fig. 8 , respectively.

E. Task 5: Arms Up and Upper Body Manipulation

This motion evaluates arms and waist capability in manipulating a 5 Kg object held by the hand. The first aim of this task is to check the arm capability in manipulation. In

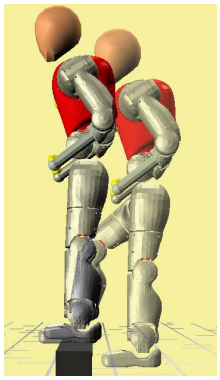

Figure 5. Step Up

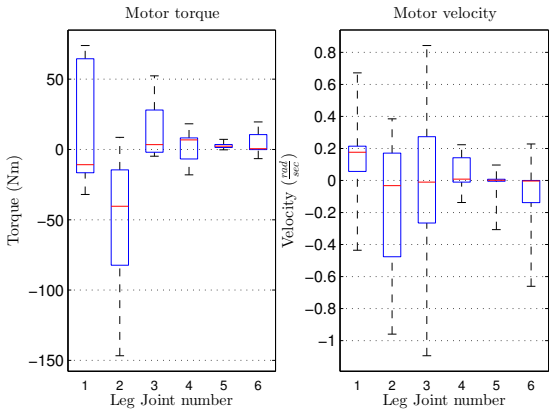

Figure 6. torque-velocity distributions of step up motion. Joints 1, 2 and 3 refer to HP, K and AP of right leg and 5, 4, 6 refer to HP, K and AP of the left leg.

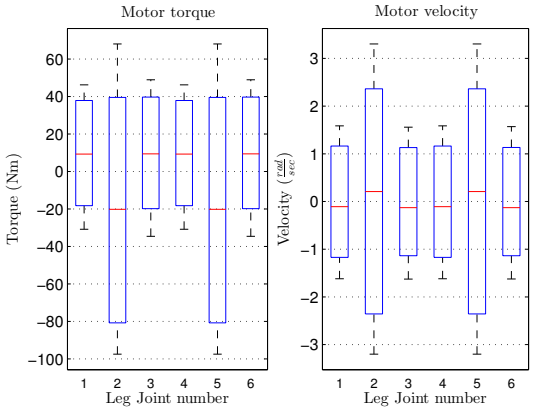

Figure 7. torque-velocity distributions of symmetric squat (both legs). Joints 1, 2 and 3 refer to HP, K and AP of right leg and 5, 4, 6 refer to HP, K and AP of the left leg.

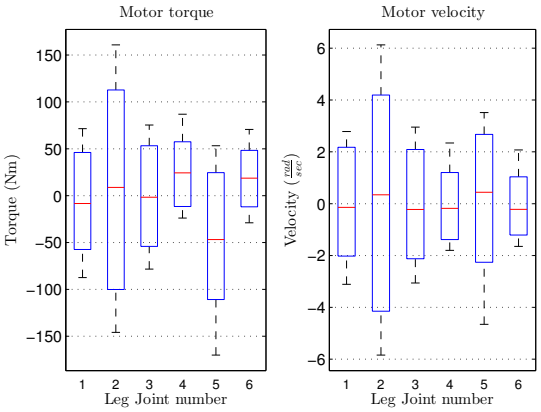

Figure 8. torque-velocity distributions of squat with one leg. Joints 1, 2 and 3 refer to HP, K and AP of right leg and 5, 4, 6 refer to HP, K and AP of the left leg.

addition to the arm torque requirements, a large torque is placed on the waist motors due to larger lever arm. A single waist motor should tolerate the whole weight of upper body and its dynamic torques. Similar graphs are obtained for this task, as presented for the previous tasks, but summarized in section IV-B.

F. Task 6: Walking and Balancing Locomotion

Walking is an essential simulation to be used in the design. The torque-speed distributions for COMAN walking with speed of 0.32 ($\frac{m}{sec}$) are shown in Fig. 9. It is evident that the knee has the highest torque and speed during walking which is partly due to bent knee walking. In addition, HR joints show higher torques compared to the pitch DoFs. Also the AP, K and HP joints has the highest velocities as expected.

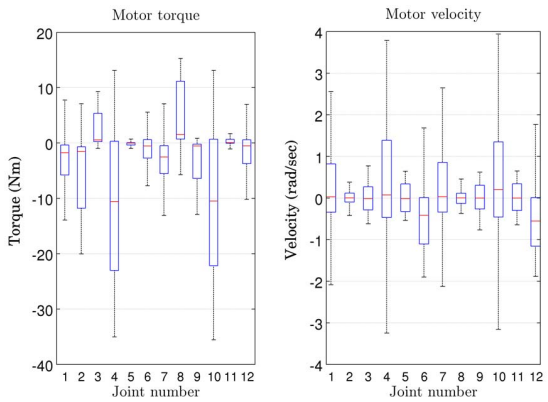

Figure 9. Torque-velocity distributions of walking with COMAN. The joints 1-6 correspond to HP, HR, HY, K, AR, AP of right leg and joints 7-12 corresponds to the left leg with the same kinematic order.

IV. Design Requirement Based on Simulation Study

The dimensions of the robot are chosen based on the requirements of the rescue operation tasks described in section III. In other words, to be able to perform the tasks for instance in a power plant, the robot must at least have anthropomorphic size. In designing the robot, we tried to reduce the weight of the robot since the robot must perform continuous tasks for at least 30 minutes using on-board battery. Besides, light weight (particularly legs and arms) gives a lot more benefits such as agility. Hence, the estimated height and weight of robot is 160mm including head, and 52kg. Based on the torque-speed graphs presented in section III, we will select different parts.

In this section, first the design of legs, arms and head is discussed and then the method used for selecting the passive compliant elements is described.

A. Transmission Selection

The ratio of harmonic drives heavily depends on the requirement of back-drivability of the joints. It was tried to reduce the gear ratio to ensure more back-drivability (based on the no load back driving torque provided in the manufacturer data). However, the torque profiles are significant in most of the joints, it will lead to very high power density motor if the gear ratio is small. Due to the limitation of the motor characteristic, the gear ratio is chosen as 100 for joints requiring more back-drivability (with no load back driving torque of 4.5 Nm for CPL-20 harmonic drive) to match with the lightest possible motor torque curve. For joints that do not require much back-drivability such as arms, waist yaw, waist roll, the gear ratio is set to 160 to allow choosing lighter motors, while the no load back driving torque is 5.8 Nm for CPL-20 harmonic drive.

B. Leg & Arm Motor Selection

Based on the presented torque-speed curves for different tasks, a short summary for each joint of legs is given in Table I. Among the large amount of data from simulation, the worst case for each joint in all tasks is selected and presented in the Table. Fig 6 (stepping on obstacle) clearly illustrates the situation when knee joint (joint 4) needs the highest power (torque times speed). The situation does not happen frequently but considering the heat from electronic parts which we encountered, the torque profile of this test is still considered to prevent failure of long time operation of motor. The maximal continuous torque is calculated as root mean square of most severe continuous torque during 2 seconds. This is quite conservative but it can help with unexpected motions which do frequently happen in outdoor environments. The peak torque and the continuous torque of the motor as well as the gear must be bigger than the torques listed in Table I. In this work, the nominal motor speed for roll and yaw joints before reduction is about 2000

rpm. The knee hip pitch and ankle pitch joints require the highest speed (around 5000 rpm) in walking ($0.32\ \frac{m}{sec}$ which is 0.64 leg length per second). Other joints do not require such high speeds.

Table I
SUMMARY OF LOWER BODY JOINTS REQUIREMENTS, (TORQUES IN NM).

Joint	Max continuous torque	Peak torque	Task
WP	50	90	Task 5
WR	20	40	Task 5
WY	8	10	Task 5
HP	50	55	Task 3, 4
HR	20	35	Task 6
HY	20	40	Task 6
K	60	100	Task 4
AR	1	11	Task 4
AP	25	40	Task 6

In summary, Table II provides the max continuous and peak torque for the upper-body (Arms & Waist). This data is used to size the upper-body joints.

Table II
SUMMARY OF UPPER-BODY JOINTS REQUIREMENTS, (TORQUES IN NM).

Joint	Max continuous torque	Peak torque	Task
SP	35	60	Task 5
SR	35	60	Task 5
SY	20	25	Task 5
E	35	44	Task 3, 4

C. Head Design

Anthropometric approach is used for preliminary decision on the head's size. Then the head geometry is revised according to the expected speed/torque performances and requirements. The head position also depends on the kinematic chain type of the whole head mechanism. The vision system includes 2 stereo-cameras and a laser scanner. Humanoid must be able to look around by turning the head from left to right 2π rad (π rad left and π rad right) and 0.35 rad up and $\frac{\pi}{2}$ rad down with respect to the horizon line. These requirements lead to a 2 DOF mechanism (yaw and pitch).

Stereo-cameras must be capable of monitoring feet of the humanoid by looking perpendicularly to the ground. To do so a pigeon-like scheme is chosen for the pitch axis which is perpendicular to yaw axis. As shown in Fig. 10, the head is pivoted to the neck to provide the pitch motion. Moreover, the yaw provides a full clockwise rotation for the neck. The total mass of the head is considered approximately to be 3.5 kg in the dynamic analysis. The pitch and yaw motors of the head should provide π $(\frac{rad}{sec})$. Two methods can be applied to generate joint level motion of the yaw and pitch namely smooth rotation trajectory and bang-bang acceleration approaches. Joint torques are calculated via Robotran based on these two motion generators. In the smooth trajectory approach a fifth order polynomial is suggested for the angle

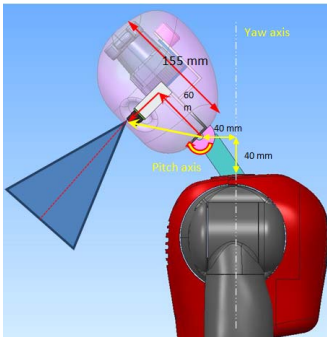

Figure 10. The head and neck design

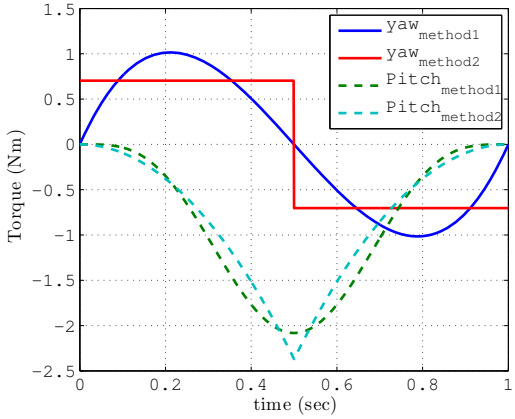

Figure 11. Head torques computed using the smooth and bang bang methods.

or rotation. The six unknown parameters could be found by specifying three initial conditions ($\theta(0) = 0$, $\dot{\theta}(0) = 0$, $\ddot{\theta}(0) = 0$) and three final conditions ($\theta(1) = \pi$, $\dot{\theta}(1) = 0$, $\ddot{\theta}(1) = 0$). The acceleration of rotation in the bang-bang approach is:

$$\ddot{\theta} = \begin{cases} +4\pi & t < 0.5 \\ -4\pi & t \geq 0.5 \end{cases} \quad (1)$$

This basically means rotating the head π rad in 1 second with peak velocity of 2π $(\frac{rad}{sec})$ .The simulated torque and velocity of yaw and pitch motors are plotted in Fig. 11. In summary, after considering friction and stiction at the joints, a motor and gearbox (ratio 100) with 4-6 Nm is sufficient for the neck.

D. Compliance Selection

Recent works [15] and [16] suggest numerical methods based on trial and error for compliance selection in designing compliant humanoids. However, for a multi degree of freedom humanoid like COMAN, these processes demand a tedious work and is undesirable. Therefore, [5] suggests an multi-body optimization method that maximizes the stored energy in joint springs and places an inequality constraint

on natural frequencies of the system and stiffnesses range. The cost function of the optimization is:

$$min(\frac{1}{\Sigma E_i}) \tag{2}$$

where E_i denotes the potential energy stored in the i joint of the leg when the torque applied by the joint is τ_i. Since the $E_i = \frac{\tau_i^2}{2k_i}$ so the cost (2) can be written in the expanded form:

$$E_i = \frac{2}{\tau_i^2 \Sigma \frac{1}{k_i}} \tag{3}$$

The joint stiffnesses should not excite the natural frequencies of the system and should be larger than trajectory and control bandwidths, $\forall \omega_i : \omega_i > \alpha \omega_b$ where ω_i is i natural frequency of the robot, ω_b is the desired bandwidth and α is a scaling parameter. Moreover, inequality constraints $k_{min} < k_i < k_{max}$ are placed to bound the desired stiffness.

The initial stiffness values are chosen as 500 $(\frac{rad}{sec})$ for AP, K, HP joints and 300 $(\frac{rad}{sec})$ for the upper body compliant joints. The hip and ankle roll joints are only connected with a gearbox. Further fine tuning of these values are required using experimental results.

V. Conclusion

In this paper, a compliant joint dynamic simulator was used to quantify the torque-speed requirement for each joint of the humanoid robot. In summary, with bended knee walking, the torque of knee joint is the most serious. Moreover, knee torque is demanded in most severe tasks such as moving objects, stand up, quadruped posture, etc. In addition, the representative tasks gave a quantitative estimate of the required torque data at other joints of the robot. In terms of compliance selection, an optimization method was used to tune the passive compliance of each joint. A new high performance humanoid robot is starting to be built using the data obtained from this study.

Acknowledgment

This work is supported by the ICT-248311-AMARSI and the FP7-ICT-2013-10 WALK-MAN European Commission projects.

References

[1] (2013), DARPA Robotics Challenge website, [Online]. Available http://www.theroboticschallenge.org/.

[2] S. Lohmeier, T. Buschmann, M. Schwienbacher, H. Ulbrich, and F. Pfeiffer, "Leg design for a humanoid walking robot", in Proc. of 6th IEEE-RAS Int. Conf. on Humanoid Robots, 2006, pp. 536-541.

[3] D. Hobbelen, T. de Boer, and M. Wisse, "System overview of bipedal robots flame and tulip: Tailor-made for limit cycle walking", in Proc. of IEEE/RSJ Int. Conf. on Intelligent Robots and Systems, Nice, France, 2008, pp. 2486-2491.

[4] D. Wollherr. Design and Control Aspects of Humanoid Walking Robots. PhD thesis, Technische Universitat München, 2005.

[5] N. Tsagarakis, S. Morfey, G. Medrano-Cerda, Z. Li, and D. G. Caldwell, "Compliant humanoid coman: Optimal joint stiffness tuning for modal frequency control", in Proc. of IEEE Int. Conf. on Robotics and Automation, Karlsruhe, Germany, 2013.

[6] EU project Whole body Adaptive Locomotion and Manipulation (Walkman), [Online]. Available http://walk-man.eu/

[7] H. Dallali, M. Mosadeghzad, G. Medrano-Cerda, N. Docquier, P. Kormushev, N. Tsagarakis, Z. Li, D. Caldwell, "Development of a Dynamic Simulator for a Compliant Humanoid Robot Based on a Symbolic Multi-body Approach", in Proc. of Int. Conf. on Mechatronics, Vicenza, Italy, February 27 - March 1, 2013.

[8] H. Dallali, M. Mosadeghzad, G. Medrano-Cerda, N. Tsagarakis, D. Caldwell, "A Dynamic Simulator for the Compliant Humanoid Robot COMAN", in Proc. ICRA Wokrshop on Developments of Simulation Tools for Robotics and Biomechanics, Karlsruhe, Germany, May 10, 2013.

[9] J. C. Samin and P. Fisette, "Symbolic Modelling of Multibody Systems", Solid Mechanics and its Applications, 1st ed.: Kluwer Academic Publishers, 2003.

[10] G. A. Medrano-Cerda, H. Dallali, M. Brown, N. G. Tsagarakis, and D. G. Caldwell, "Modelling and Simulation of the Locomotion of Humanoid Robots", in Proc. of the UK Automatic Control Conf., Coventry, UK, 2010.

[11] J. Lee, H. Dallali, N. Tsagarakis and D. Caldwell, "Robust and Model-Free Link Position Tracking Control for Humanoid COMAN with Multiple Compliant Joints", To Appear in Proc. of IEEE Int. Conf. on Humanoid Robots, Atlanta, Georgia, USA, Oct. 15-17, 2013.

[12] H. Dallali, P. Kormushev, Z. Li, D. Caldwell, "On Global Optimization of Walking Gaits for the Compliant Humanoid Robot, COMAN Using Reinforcement Learning", Journal of Cybernetics and Information Technologies, vol. 12, no. 3, pp. 39-52, 2012.

[13] A. Del Prete, F. Nori, G. Metta, and L. Natale, "Partial Force Control of constrained Floating-Base Robots", submitted to IEEE Int. Conf. on Robotics and Automation (ICRA), Hong Kong, China, 2014.

[14] H. Dallali, (2013), COMAN Simulator Repository, [Online]. Available https://github.com/HDallali/ComanSimulator

[15] J. Hurst. "The electric cable differential leg: A novel design approach for walking and running". Journal of Humanoid Robots, 8(2):301 321, 2011.

[16] N.G. Tsagarakis, M. Laffranchi, B. Vanderborght, and D.G Caldwell, "A compact soft actuator for small scale robotic systems", in Proc. of IEEE Int. Conf. on Robotics and Automation, Kobe, Japan, 2009, pp. 4356 4362.